17th World Conference on Earthquake Engineering, 17WCEE
Sendai, Japan - September 13th to 18th 2020

OVERVIEW OF EXPERIMENTAL PROGRAM ON CAST-STEEL REPLACEABLE YIELDING LINKS IN ECCENTRICALLY BRACED FRAMES

P. Mortazavi [1], E. Lee [2], J. Binder [3], M. Gray [4], O. Kwon [5], C. Christopoulos [6]

[1] *Ph.D. Candidate, Department of Civil and Mineral Engineering, University of Toronto, pedram.mortazavi@mail.utoronto.ca*
[2] *M.A.Sc. Student, Department of Civil and Mineral Engineering, University of Toronto, edenn.lee@mail.utoronto.ca*
[3] *Project Engineer, Cast Connex Corporation, j.binder@castconnex.com*
[4] *Executive Vice President, Cast Connex Corporation, m.gray@castconnex.com*
[5] *Associate Professor, Department of Civil and Mineral Engineering, University of Toronto, os.kwon@utoronto.ca*
[6] *Professor and Canada Research Chair, Department of Civil and Mineral Engineering, University of Toronto, c.christopoulos@utoronto.ca*

Abstract

The response of Special Moment Resisting Frames (SMRFs) is often accompanied by large drifts owing to their inherent flexibility, while Special Concentrically Braced Frames (SCBFs) develop substantial forces in their response due to their high stiffness. Steel *Eccentrically Braced Frames (EBFs)*, which have been proposed as lateral load resisting systems for seismic applications since the early 1970s, provide an attractive alternative to more commonly used systems in steel structures as they combine the advantages of both systems. Shear links in EBFs are more common because of their advantages compared to flexural links. About a decade ago special attention was given to *Replaceable Links* in EBFs to facilitate fabrication, post-earthquake repairs, and ease of the design procedure. While having proven to be an effective seismic force resisting system (SFRS), the response of conventional EBFs and replaceable EBF links with conventional steel sections have stringent welding requirements for connections and can be prone to undesirable limit states such as web fracture close to web stiffeners, local buckling, and lateral torsional buckling. An experimental program is currently on going at the University of Toronto on the experimental validation of a new generation of energy dissipative links, known as *Cast Steel Replaceable Links*, in EBFs. The proposed links use *Steel Casting* technology to achieve a better response in terms of ductility and low-cycle fatigue life and to address the drawbacks associated with the response of conventional EBF links. In the first phase of the experimental program, the response of the proposed links is validated through a set of component-level reversed cyclic tests, using a universal axial testing frame. In the second phase, the system is tested at the system-level as part of a one-story steel frame. This paper provides an overview of the proposed system and outlines the experimental program that is currently in progress at the University of Toronto. The design of the experimental setups, instrumentation, and preliminary test results are presented. Preliminary observations are reported and further experimental studies that are underway are briefly outlined.

Keywords: Eccentrically Braced Frames, Steel Casting, Energy Dissipative Links, Hysteretic Dampers, Steel Structures

1. Introduction

Since the first introduction of eccentrically braced frames (EBFs) in the mid-1970s, they have increasingly gained acceptance and have been used in steel construction. EBFs are unique for their reliable lateral stiffness and their excellent energy dissipation capacity. The former is due to the presence of diagonal braces and the latter is achieved through stable yielding of the energy dissipative link during seismic events. Initial studies on conventional links, which was mainly a segment integral to the floor beam, were focused on understanding the behaviour of wide flange sections under cyclic loading. For links using conventional steel sections, depending on the link length, links are classified as shear critical or flexural link [1-2]. Early experimental studies established the advantages of shear critical links over flexural links [1-3], as they offer uniform plasticity over the entire web. This is contrary to flexural links, which only develop local plastic hinges at their ends. This led to many studies on the behaviour of shear links. The studies have shown that incorporating web stiffeners is necessary in shear links in order to prevent web buckling and achieve a stable energy dissipation [1-3]. Alternative link sections were also studied, including built-up sections with welded flanges to webs and tubular

links which were experimentally validated to have a promising performance [4-5]. The effects of local buckling and the use of A992 steel were also studied to provide improvements in the AISC Seismic Provisions [6] for seismic web and flange compactness requirement for the links. In most studies, web fracture close to stiffeners was the ultimate failure mode of shear links [3,5-6].

The design procedure for conventional links requires the floor beam to yield in the link region while being capacity protected in the area outside of the link. In addition to making the design process iterative, this often leads to overdesigned structures and increased overall cost. Replaceable links were an innovative solution that would allow the designer to decouple the yielding link from the floor beam. Replaceable links also facilitate ease of construction and replacement following a major earthquake [7]. Since their development, their design is adopted by relevant design guidelines [8] and they have gained attention from the engineering community. In particular, they have been used in building constructions as part of the efforts for rebuilding of Christchurch [9].

Despite the improvements in design procedure and performance of EBFs, the replaceable links are typically formed by back to back channels or W sections welded to endplates with stringent welding requirements. These links are susceptible to similar failure modes as conventional links and can only achieve maximum plastic rotations of 0.08 rad [7]. This paper presents a novel *Cast Steel Replaceable Link* for use in EBFs to address these drawbacks and outlines the experimental program that is currently in progress at the University of Toronto for validating the performance of the proposed system.

2. Cast Steel Replaceable Links in EBFs

The advantages of *Steel Casting* technology in structural design have been outlined by several previous studies. Steel casting allows for the use of free-flowing geometries and customized material chemistry which can enhance structural response attributes such as ductility and low-cycle fatigue life. The customization associated with steel castings can help to control stress concentration and residual stresses [9] and can lead to more economical design solutions for parts requiring complex geometries [10] and/or mass-produced components. Given these advantages, steel castings have been used in earthquake engineering research and practice in recent years and cast steel energy dissipative fuses have been proposed, developed, and used in construction [11-17].

The use of steel castings in EBFs was first studied by Tan and Christopoulos [18] through finite element (FE) analyses. Several geometries and designs of cast steel links were investigated with the primary goal of having simultaneous distributed flexural yielding, similar to cast steel yielding connectors [16]. The final proposed link by Tan and Christopoulos was formed by a hollow box with a tapered width, which distributed the plastic strains along the yielding portion of the link. The choice of using a hollow section was primarily aimed at better controlling the lateral torsional buckling [5] and to remove the necessity of having lateral supports for links in EBFs.

In the present study, the design of the previously proposed cast steel links [18] is modified. Height, width, and the thickness of the hollow section are tapered to achieve optimized geometry over the length of the link such that a constant cross-sectional area is maintained over the length of the link yielding segments, while maintaining the properties that facilitates distributed flexural yielding. With this new design, the link axial force causes uniform strains in the yielding segments. This leads to evenly distributed strains in the yielding portion of the link even under combined flexure and significant axial loads. The ratio of moment of inertia about the X axis to moment of inertia about the Y axis was kept as $I_x/I_y=0.67$, as the limit which removes the necessity of providing supports for lateral torsional buckling in tubular steel sections [18]. The geometry of the links was further optimized through extensive FE analyses to prevent local buckling and have highly increased ductility and low cycle fatigue life. The width to thickness ratio is limited to 5.0 to prevent local buckling in flanges, based on the FE analyses [19]. The middle segment of the link is designed to behave as an elastic rigid block, which connects the yielding segments.

The links are connected to the floor beam with bolted end plates. The length of the links within the set, excluding the end plates are around +/- 700 mm long. The total length of the device, including the end plates

is around +/- 850 mm. This length was chosen as a reasonable length compatible with most frame geometries in building construction. Currently, nine off-the-shelf link sizes are designed and detailed with different nominal shear capacity (V_P) to provide a range of options for design solutions. The sizes are shown in Fig. 1. The number next to the EBF, is the nominal shear capacity of the device in kips. The nominal shear capacity of each size is also shown in kilonewtons.

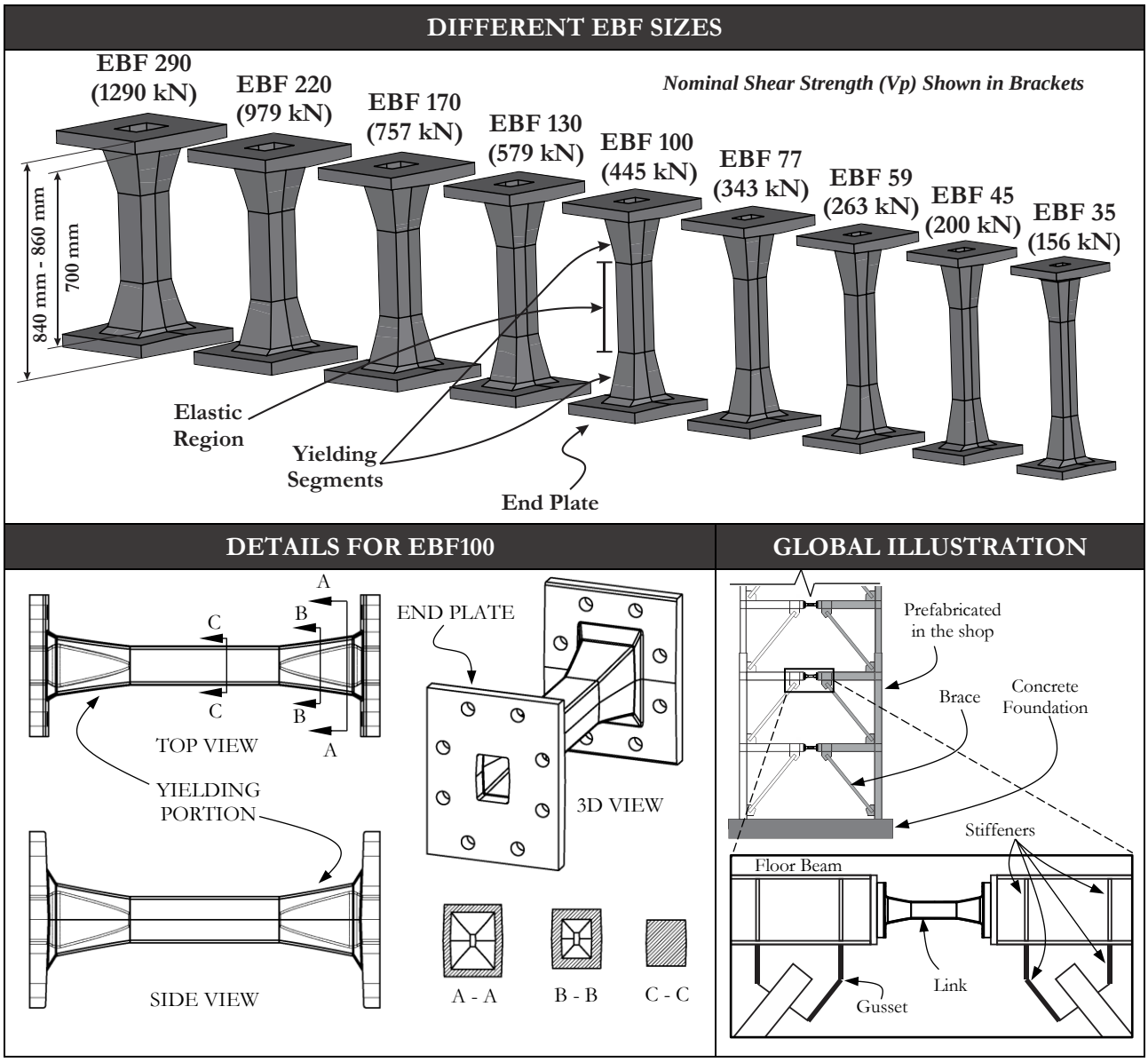

Fig. 1 – Proposed cast steel replaceable links in eccentrically braced frames

3. Experimental Program

A comprehensive experimental program is currently underway at the University of Toronto to validate the response of the proposed cast steel replaceable links in EBFs. In the first phase of the study, the link performance is validated locally through a set of reversed cyclic experiments at a component level. Five links are tested in the component setup including two EBF290s (V_P = 1290 kN), one EBF100 (V_P = 445 kN), and two EBF35s (V_P = 156 kN). Next, the performance of the proposed links is validated on a system level and through reversed cyclic tests within a one-storey frame setup, where two EBF100s are tested within the frame. This forms the first part of the experimental program, which is covered in this paper.

3.1 Component-Level Experimental Validation

3.1.1 Experimental Setup Design

The test setup for the component-level tests is shown in Fig. 2 from several views. The test setup is formed by a universal axial testing frame with a load capacity of 2700 kN and a displacement capacity of +/- 150 millimetres. The blue loading frames are designed to put the specimen under a uniform shear demand and a linear moment diagram similar to the loading condition that the link experiences in an EBF frame. The loading frames are post-tensioned together using high-strength bolts and connected to the universal testing frame with pins. The pins were fabricated with very small tolerance to limit any slackness. In the initial cycles, a pin slackness of only 0.2 mm was observed. The specimen loading beams have two endplates with different hole patterns and detailing at each end to allow for testing of several link sizes. The member sizes, endplate details, and fasteners were initially sized using first principles and then confirmed and optimized using FE analyses.

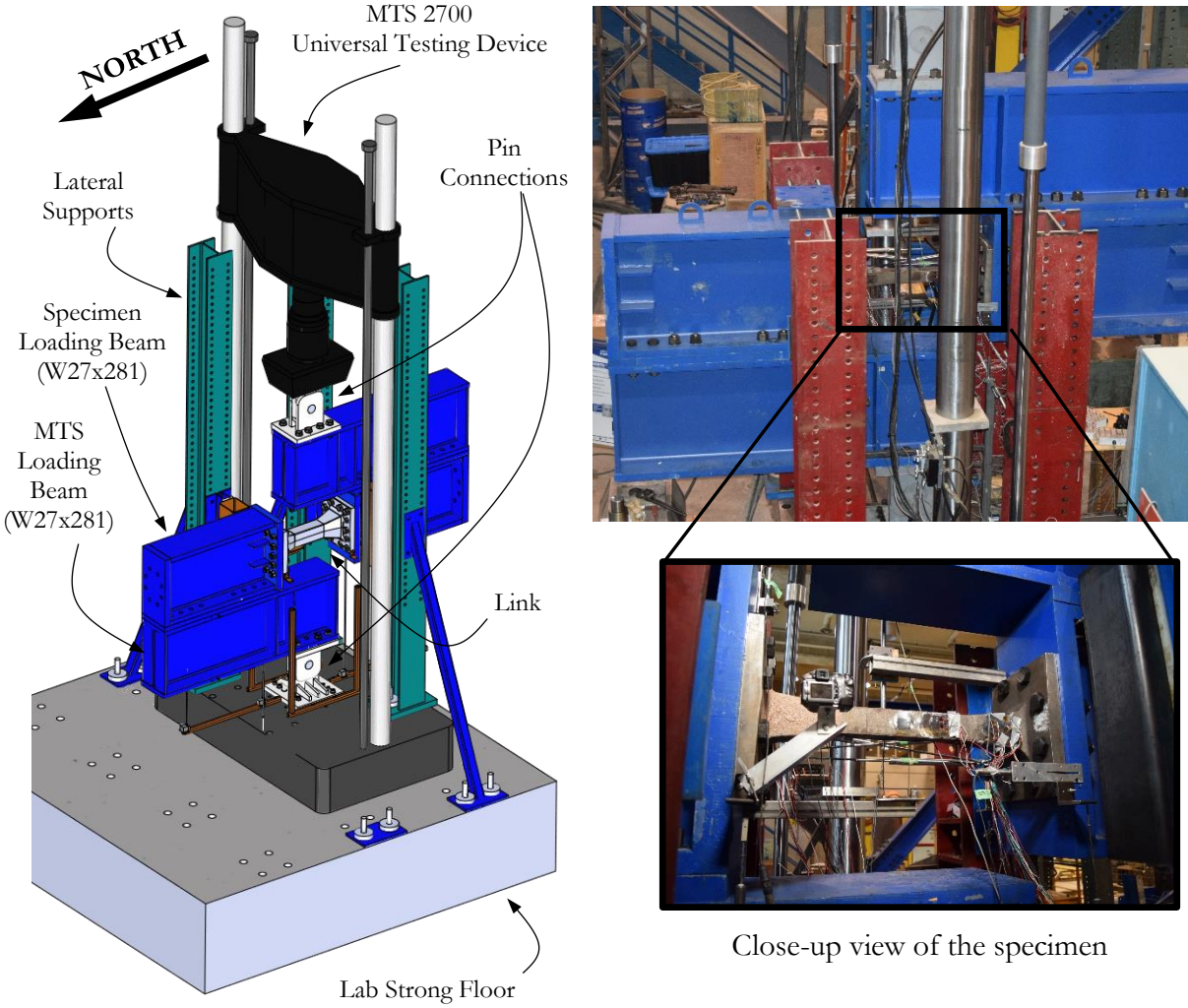

Fig. 2 – Component-level experimental validation

3.1.2 Instrumentation

The component-level tests are monitored using a variety of sensors. High-capacity strain gauges and strain rosettes are used to monitor the strains in the specimen's yielding flanges and webs. In addition, several strain gauges and rosettes are used in the elastic region of the link to obtain the strain diagram along the length of the specimen. Fig. 3 shows some of the displacement sensors used in the component-level experimental validation. Four linear potentiometers (D1, D2, D3, and D4) are used to measure the specimen's axial elongation and its

rotation due to deformation of the diagonal sensors. Linear variable differential transformers (LVDT) are used to measure the movement of the end plates with respect to the setup base (D5 and D6). D5 and D6 LVDTs are used on both east and west sides of the setup. This facilitates monitoring any undesired torsion or twisting of the specimen. An LVDT (D7) is used to measure the total vertical deformation of the link specimen, which can be related to its tangential rotation. This is the rotation with which the loading protocol is applied. Four spring potentiometers are used to monitor the movement and rotation of the loading beams. SP1 and SP2 are used for the lower loading beams, while SP3 and SP4 are used for the upper loading beams. A linear potentiometer is used at the pin location (LP2) to measure the slack in the pin, if any. Two small LVDTs are also used to monitor potential undesired end plate slip and gap opening during the experiment, as can be observed in the close-up view of the specimen in Fig. 2. Lastly, a digital image correlation (DIC) method is used to measure the strain field in the specimen. A camera is attached to the specimen using a rigid arm that moves with the specimen. The camera is set up to take pictures at specific intervals, so that the images can be used for the DIC application.

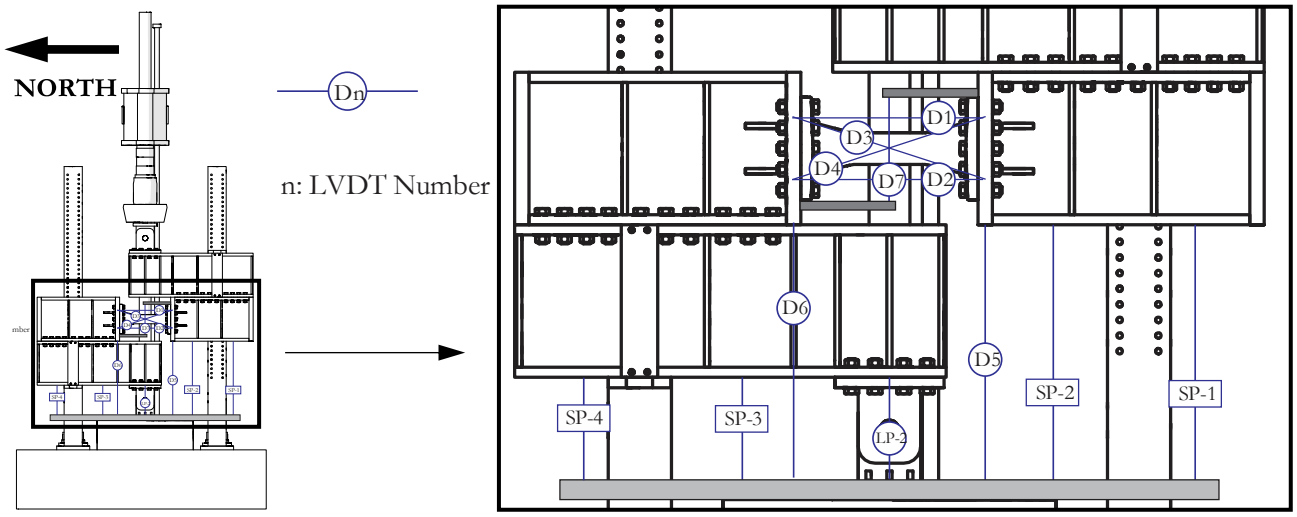

Fig. 3 – Component-level experimental validation instrumentation

3.1.3 FE Results and discussion

The main purpose of the component-level experimental validation is to assess the performance of an isolated link. As such, FE models were generated, and analyses are performed in order to optimize the design of the setup and to ensure that the restraints that were imposed on the link by the setup are minimal. An FE model of the link alone and without the experimental setup was also developed, referred to as the standalone model, to provide a basis for comparison.

The cast steel material was defined using the cyclic hardening parameters in ABAQUS. The kinematic hardening parameter, C_1, was taken as 4000, γ_1 taken as 28, Q_∞ taken as 50, and b was taken as 2 as suggested by previous studies [20]. The yield stress of the cast steel material is 295 – 300 MPa. However, R_y of 1.1 is assumed and the yield stress for the cast material is increased to 328 MPa in order to make the FE analysis conservative. The material for A490 bolts is defined using an elastoplastic material behaviour with a yield stress of 1040 MPa. G40.21-W300 and G40.21-W350 steel grades are defined using elastoplastic materials with yield stress values of 300 MPa and 350 MPa. For all steel materials the modulus of elasticity is taken as 200000 MPa and the Poisson ratio is taken as 0.3. All fabricated steel elements are meshed using C3D8R 8-node linear brick elements with reduced integration and hourglass control. The link is meshed using C3D10 10-node quadratic tetrahedron elements. The interaction between the specimen loading beam and the MTS loading beam, interaction between the bolt shank and the steel holes, and the interaction between the bolt head/nut and steel members is modelled using a tangential behaviour with a friction coefficient of 0.3 and a "Hard" Contact normal behaviour. The link end plates are tie constrained to the test setup end plates, since end plates have shown satisfactory performance in previous experiments [7]. The bolt post-tension (PT) force is

modelled for 1-1/2" A490 bolts connecting the MTS loading beam to the specimen loading beam. The bolt PT force is propagated using the *fixed at current length* method during the analysis. The weight of the setup is also included in the analyses to assess its effect on the response. Both X and Y movements are restrained at point A, while only movement in the X direction is retrained at point B. The rotation degree of freedom (DOF) is free at both A and B to represent the setup boundary conditions. The free DOFs are shown with green, while the restrained DOFs are shown with black.

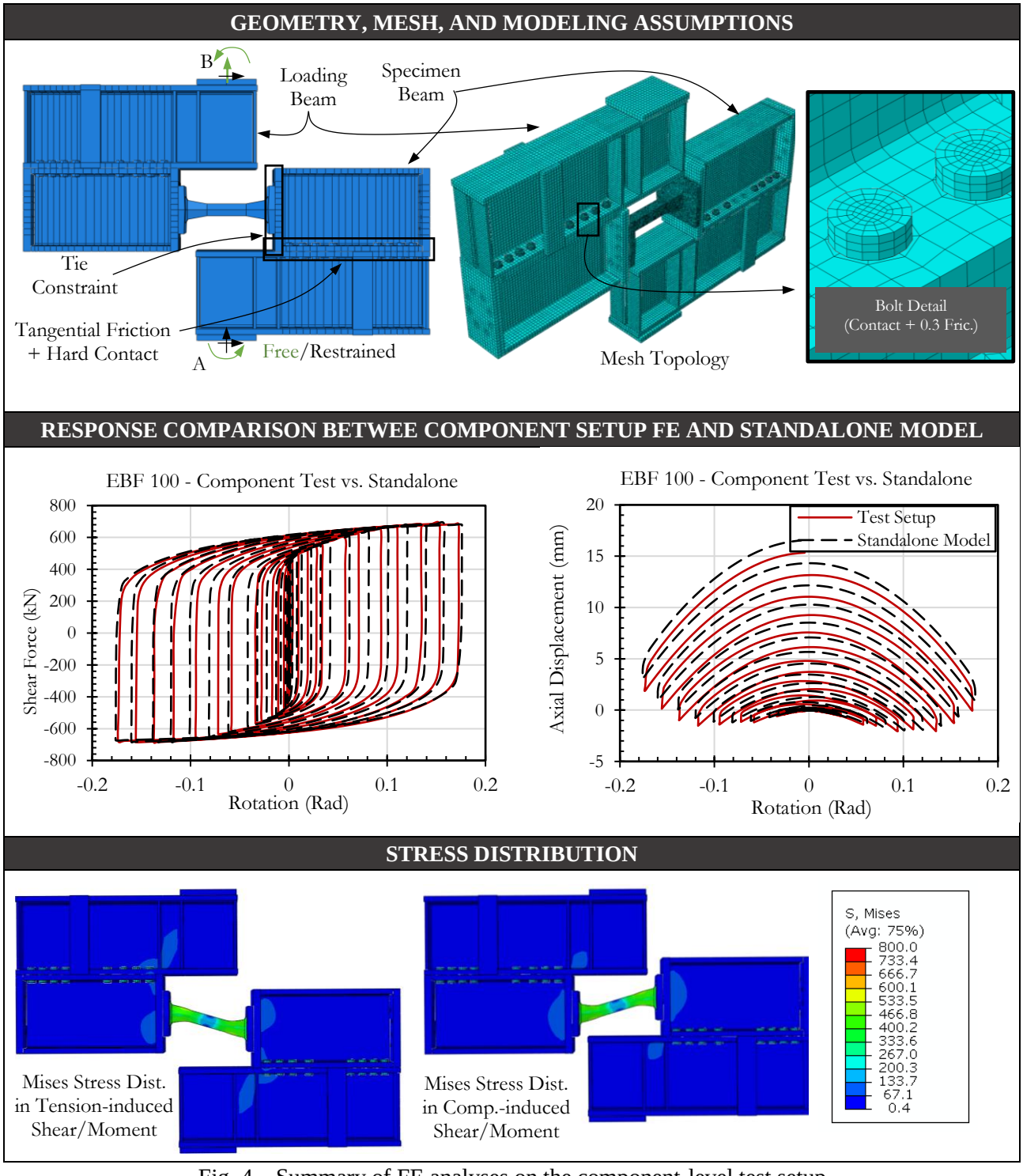

Fig. 4 – Summary of FE analyses on the component-level test setup

The AISC 360-41 displacement protocol for EBF links is applied to the setup [21]. After design optimizations, the response was compared with FE results from the standalone model under the same protocol. FE analyses were performed for all three sizes of EBF290, EBF100, and EBF35. Results and figures from the EBF100 FE analysis are presented in Fig. 4. As can be observed, the FE analyses indicated that the experimental setup simulates the free conditions for the link well and the setup achieves its intended goal.

3.2 Frame-Level Experimental Validation

3.2.1 Experimental Setup Design

Two EBF100 (V_P = 445 kN) links will be tested in the frame setup shown in Fig. 5: once without the slab, and once with the slab. This enables a direct comparison between the behavior of specimen without the slab and the composite action of the two in a global system, and an assessment of the effects of slab action on the link behavior.

The frame has a column-to-column distance of 6.10 m (20 ft) and a height measured from the pin supports of the columns to the floor beam centreline of 2.74 m (9 ft). The link has a total length of 838 mm (33 inches) including the endplates which results in an angle between column and brace of 43.8º. Two actuators, each with a capacity of 1000 kN (225 kips), are connected to transfer beams which are then directly attached to the north floor beam of the frame. This configuration leads to having moment and shear forces on the link accompanied by large axial forces. Each full cycle will experience tension in half a cycle and compression in the other half. This allows critical review of the effect of axial loads on the response of cast steel replaceable links.

The transfer beam is designed to have a stiff response to ensure no additional deformation develops between the actuator and the floor beam. Lateral supports are provided to avoid any undesired out-of-plane movements. The columns are attached to the base plate on the strong floor as pinned supports. Brace-to-column and brace-to-beam connections are detailed with gusset plates with stiffeners. All members within the setup are designed to remain elastic under the force capacity of the actuators, with a reasonable safety margin.

Fig. 5 – Experimental Setups

The floor slab is constructed using a standard 20-gauge cold-formed metal deck with a 38.1 mm (1.5 in) and 152.4 mm (6 in) rib height and width, respectively, and a slab topping of 95.3 mm (3.75 in). The concrete

has a 28-day compressive strength of 30 MPa (4,350 psi) and is reinforced by a prefabricated welded mesh of 152x152 MW9.1/9.1 (6x6 W1.4/1.4). This reinforcement is equivalent to the minimum 0.2 percent transverse and longitudinal temperature reinforcement per linear meter. The slab is 1,145 mm (3.75 ft) wide and 2,740 mm (9 ft) long, which covers about 3.27 times the length of the link. Composite action is developed using shear stud connectors measuring 114.3 mm (4.5 in) above the bottom of the metal rib. For ease of construction, the slab is cast on the ground with embedded headed threaded rods used as shear connectors. The threaded part of the headed studs remains exposed below the concrete slab after casting. The geometry of the studs matches the holes on the floor beam. After the 28-day strength is developed, the slab is placed on the floor beams. The shear connectors are inserted through the prefabricated holes on top flange of the floor beams, then fastened with a nut under the flange to avoid slip, and to ensure full shear transfer from the beam to composite floor slab. The shear connectors start at 1d away from either ends of the link, where d represent the depth of the link. Each rib has two 9.53 mm (0.375 in) shear connectors to develop full capacity for composite action, as per CSA S16-19 [8].

3.2.2 Instrumentation

The frame will be subjected to quasi-static cycles of lateral displacement in the plane of the frame to impose cyclic link rotation. The loading protocol in outlined Section K2.4c of ANSI/AISC 341-16 [21] which specifies the number of cycles per link rotation. To monitor the link rotation and axial deformation, two linear potentiometers are diagonally installed on one side of the link, as well as two linear potentiometers. Strain gauges and rosettes are used to monitor the strains in the link. Relative link end displacement is also measured using an LVDT. The strains of beams, braces, and columns are measured at each end and middle of the elements using strain gauges, in order to find the forces. LVDTs installed at brace-to-column and brace-to-beam connections track any slip at the connections. The overall frame drift is determined by two LVDTs measuring the lateral displacements at the column pin and centerline of floor beam. LVDTs are also placed on both sides of the link to measure the relative slip between the slab and floor beam. The instrumentation of the frame setup is roughly shown below.

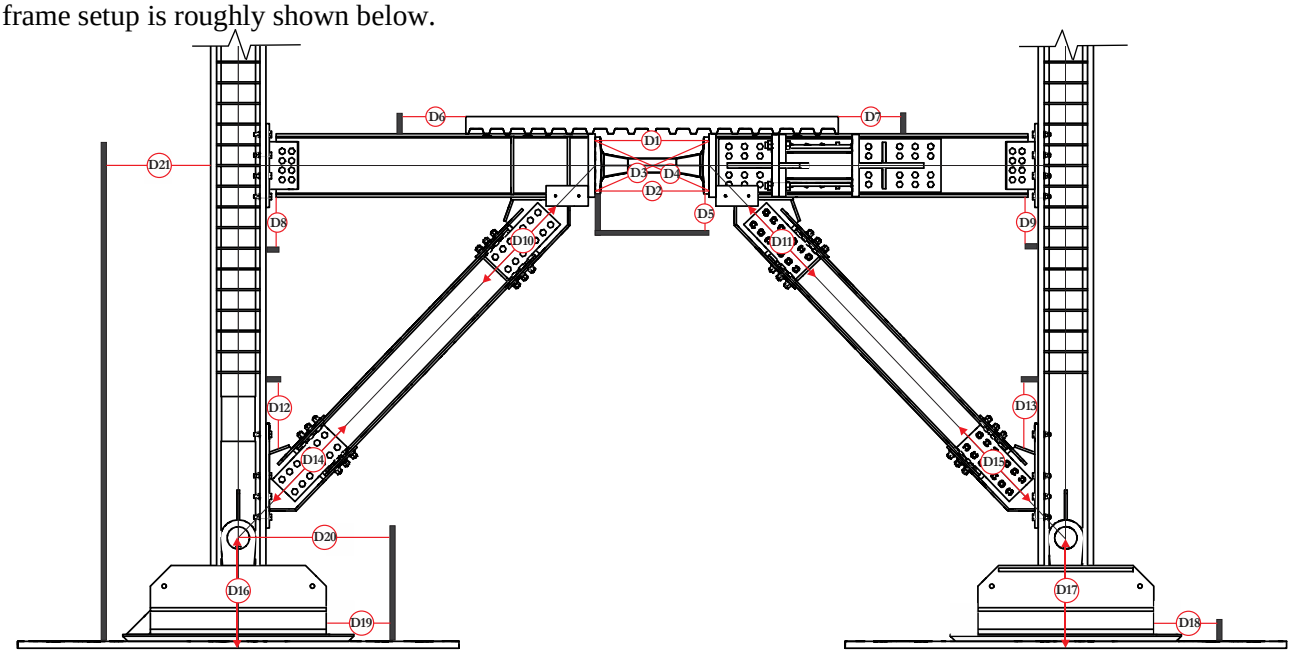

Fig. 6 – Frame-level experimental validation instrumentation

3.2.3 FE modeling and discussion

As part of the design for the frame setup, nonlinear FE models were developed for the EBF100 and the frame setup to investigate the link behavior in the presence of the concrete slab and when subjected to lateral displacement from one side or both sides of the frame. This investigation was conducted primarily to predict the behavior of the link in composite action with a cracked slab section under high cyclic rotations, and also

to compare the link response when loaded on one side versus both sides of the frame. It also allows to investigate the level of damage that can be expected in the slab at different frame displacement levels to assess the resilience of the overall system.

Fabricated steel members were modelled using the hardening parameters calibrated by Korzekwa and Tremblay [22]: kinematic hardening modulus, C_1, was taken as 8000 MPa. γ_1 was taken as 75. Q_∞ was taken as 110 MPa and b was taken as 4. G40.21-350W grade steel with a nominal yield strength of 350 MPa, a Young's modulus of 200000 MPa and a Poisson's ratio of 0.3 was considered. Ten-node tetrahedral elements with second-order shape functions (referred to as C3D10M elements in ABAQUS) were used to mesh the link.

The beams, braces, and columns were modeled using linear beam elements with consistent sectional properties and center-to-center dimensions used in the experimental setup of the frame. The ends of the floor beams are rigidly tied to the link end plate.

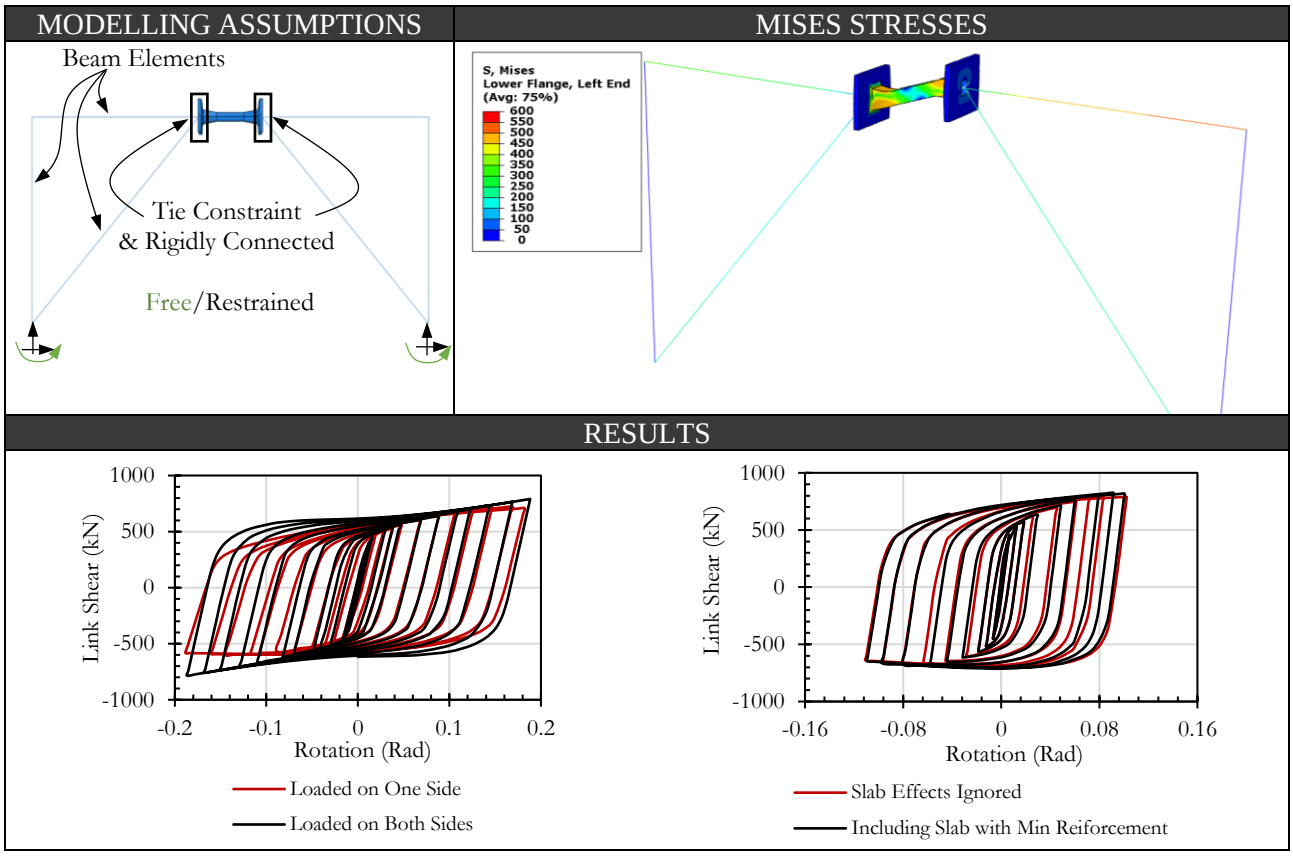

Fig. 7 – Summary of the FE analyses on the frame-level experimental setup

The frame was subjected to the loading protocol. Shear force in the link was calculated based on vertical support reactions and plotted against link rotation determined by relative link end vertical displacement and change in horizontal link length. As seen in Fig. 7, when both sides of the frame are subjected to equivalent lateral displacements, the link observes high overstrength in both positive and negative shear. Since the horizontal distance between the two nodes is fixed, the link will experience tension especially when achieving high link rotation, resulting in large overstrength in both directions. However, when the frame is subjected to lateral displacement on only one side of the frame, an imbalance of overstrength in positive and negative shear can be observed in the link, with strength deterioration on one side and increased hardening on the other side. This effect was observed in experimental testing of built-up W-section links in [7]. This behavior will be further verified and studied by the experiment when subjected to lateral displacement on one side of the frame.

The composite slab was simplified as a linear beam element with the same axial stiffness as the minimum reinforcement area required by CSA S16-19 for the slab. A beam element was defined with the same length as

the slab in the experimental setup to investigate this. The beam element representing the slab was then tied to the nodes along the frame beam by pinned connection to ensure freedom of rotation while providing axial restraint to the link. Fig. 7 plots the shear force versus rotation once without the slab, and once with the slab. As can be observed, the slab presence is not likely to affect the response of the link notably. This is something that will further be investigated during the experimental program.

4. Preliminary Verification Test Results

Preliminary results from the initial cycles of the component-level tests on the first EBF35 (V_P = 156 kN) are presented in this section. Additional results will be presented in future publications on this experimental program. The completed portion of the loading protocol is shown in Fig. 8(a). The link shear versus rotation is shown in Fig. 8(b). The same data is shown in Fig 8(c) with the rotation axis limit adjusted to rotations that are expected to be observed during the tests. As can be observed, the specimen has not sustained much yielding yet. The results of the DIC are also presented in Fig. 8(d) in terms of strain field on link's web over the yielding region, in the longitudinal direction. The strain profile matches the expected flexural strains. With increased strains, it is expected for the strain profile to have a smoother gradient.

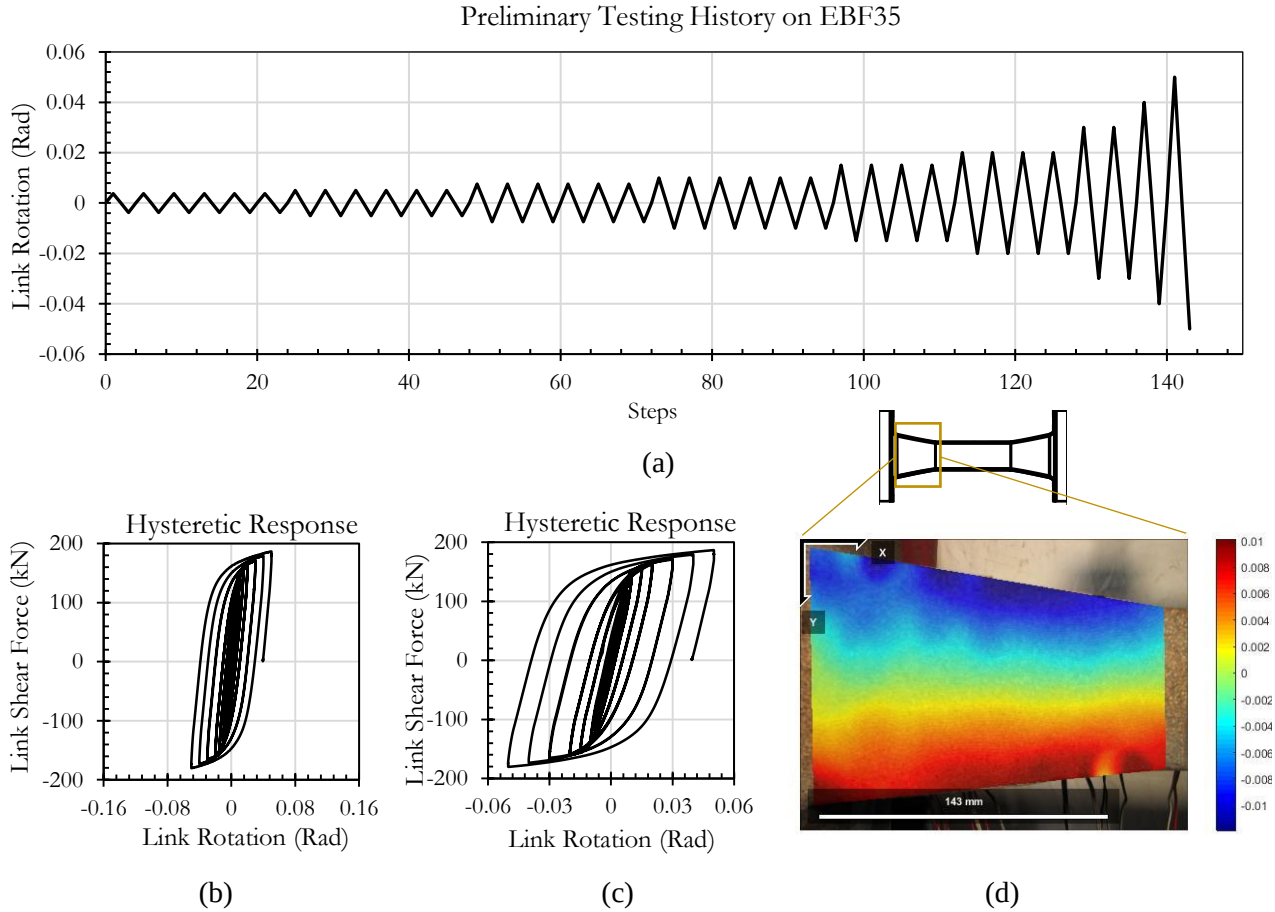

Fig. 8 – Preliminary verification test results from the component-level experimental validation

5. Future Work

After the completion of the conventional reversed cyclic tests on the component- and system-level, several hybrid simulations are planned. In the first phase of hybrid simulations, two link specimens will be tested in the frame experimental setup in a hybrid manner. These tests will be of particular interest as the EBF link

performance will be studied both locally and globally under random vibrations, while considering the effects of axial load on the link response caused by imbalanced inertia forces. These tests will be carried out using the University of Toronto Simulation (UT-SIM) Framework [23-25]. In the second phase of the hybrid simulations, the University of Toronto Ten Element Hybrid Simulation Platform (UT10) [26-28] will be upgraded and used for multiaxial hybrid simulations on the link. These experiments are of interest as the nonlinear behaviour of the yielding links will be studied thoroughly under combinations of axial loads, either caused by axial restraint or imbalanced inertia forces, and flexural moments and shear loads. These hybrid tests will further help with the development of numerical models for performance assessment of EBFs with cast steel links, and calibration of low-cycle fatigue life prediction models.

6. Concluding Remarks

This paper provides an overview of the experimental validation of cast steel replaceable links in steel EBFs. The design of previously proposed cast steel links in EBFs [18] is reviewed and current design and available cast steel replaceable link sizes are presented. The extensive FE analyses that were done during the development of the new design of EBF links showed a promising performance in terms of energy dissipation, ductility, and low-cycle fatigue life.

The first phase of the experimental program, which mainly consists of conventional reversed-cyclic tests on a component- and system-level is outlined in detail. The design, instrumentation, and FE analyses on the experimental setups are presented. It was shown that the component-level experimental setup does not impose a notable restraint on the link, and as such, can be used for understanding the response of an isolated link. Results of the preliminary component-level tests on EBF35, the smallest EBF size in the set, are presented up to rotation of 0.05 radians in the loading protocol. The results indicate that the experimental setup is performing as intended. The results up to 0.05 radians of link rotation show a stable hysteretic response for the cast steel replaceable link. The DIC results are also presented in terms of longitudinal strain fields. The strains gradient matches the expected flexural response.

7. Acknowledgements

The authors acknowledge the support of the Natural Sciences and Engineering Research Council of Canada (NSERC) [CRD 505341-2016] and Ontario Centers of Excellence [OCE VIP II -27058].

8. References

[1] Kasai K, Popov EP (1986): Cyclic web buckling control for shear link beams. *Journal of Structural Engineering*, **112** (3), 505-523.

[2] Engelhardt MD, Popov EP (1989): On design of eccentrically braced frames. *Earthquake spectra*, **5** (3), 495-511.

[3] Uang CM, Bruneau M (2018): State-of-the-art review on seismic design of steel structures. *Journal of Structural Engineering*, **144** (4), 03118002.

[4] Itani AM, Elfass S, Douglas BM (2003): Behavior of built-up shear links under large cyclic displacement. *Engineering Journal*, **40** (4), 221-234.

[5] Berman JW, Bruneau M (2007): Experimental and analytical investigation of tubular links for eccentrically braced frames. *Engineering Structures*, **29** (8), 1929-1938.

[6] ANSI/AISC 360-16: Specification for Structural Steel Buldings (2016), *American Institute of Steel Construction*, Chicago, Illinois.

[7] Mansour N, Christopoulos C, Tremblay R (2011): Experimental validation of replaceable shear links for eccentrically braced steel frames. *Journal of Structural Engineering*, **137** (10), 1141-1152.

[8] CSA S16-19: Design of Steel Structures (2019), *Canadian Standard Association*, Toronto, Canada.

[9] Bruneau, M., MacRae, G. (2017): Reconstructing Christchurch: A seismic shift in building structural systems, *The Quake Centre*, University of Canterbury.

[10] Lomax, K. B. (1982): Forging and castings. *Materials for the process industrie: papers originally prepared for a conference held in 1982*, (pp. 23-24). London: Mechanical Engineering Publications.

[11] Armitage, R. (1983): Development of cast node joints for offshore production platforms. *Solidification technology in the foundry and cast house*, (pp. 385-391). London: The Metals Society.

[12] Fleischman, R.B., Li, X., Pan, Y. and Sumer, A. (2007a): Cast modular panel zone for steel special moment frames. I: Analytical development. *ASCE Journal of Structural Engineering*. **133** (10), 1393-1403.

[13] Fleischman, R.B., Palmer, N.J., Wan, G. and Li, X. (2007b): Cast modular panel zone for steel special moment frames. II: Experimental verification and system evaluation. *ASCE Journal of Structural Engineering*. **133** (10), 1404-1414.

[14] Sumer, A., Fleischman, R.B. and Palmer, N.J. (2007): Development of a cast modular connector for seismic-resistant steel moment frames. Part II: Experimental Verification. *AISC Engineering Journal*. **44**(3), 213-231.

[15] Federico, G., Fleischman, R.B. and Ward, K.M. (2012): Buckling control of cast modular ductile bracing system for seismic-resistant steel frames. *Journal of Constructional Steel Research*, **71**, 74-82.

[16] Gray, M., Christopoulos, C., packer, J. (2014): Cast steel yielding brace system for concentrically braced frames: Concept a development and experimental validations, *ASCE Journal of Structural Engineering*, **140** (4): 04013095.

[17] Mortazavi, P., Kwon, O, Christopoulos, C., Gray., M. (2020): Four-element hybrid simulation of a steel frame with cast steel yielding connectors, *Proceedings of the 17th World Conference on Earthquake Engineering*, Sendai, Japan.

[18] Tan K, Christopoulos C (2016): Development of replaceable cast steel links for eccentrically braced frames. *Journal of Structural Engineering*, **142** (10), 04016079.

[19] Binder, J., Gray, M., Christopoulos, C., De Oliveira, C. (2017): Cast steel replaceable modular links for eccentrically braced frames. *ASCE Structures Congress*, Denver, Colorado.

[20] Zhong, C., Binder, J., Kwon, O., Christopoulos, C. (2020): Experimental and numerical characterization of ultralow-cycle fatigue behavior of steel casting, *ASCE Journal of Structural Engineering*, **146**(2): 04019195.

[21] ANSI/AISC 341-16: Seismic Provisions for Structural Steel Buildings (2016), *American Institute of Steel Construction*, Chicago, Illinois.

[22] Korzekwa, A., Tremblay, R. (2009): Numerical simulation of cyclic inelastic behavior of buckling restrained braces, *Proceedings of the Conference on Behavior of Steel Structures in Seismic Areas*, STESSA. Philadelphia, Pennsylvania, p 653-658.

[23] Huang, X., Kwon, O. (2018): A generalized numerical/experimental distributed simulation framework, *Journal of Earthquake Engineering*, DOI: 10.1080/13632469.2018.1423585.

[24] Mortazavi, P., Huang, X., Kwon, O., Christopoulos, C. (2017): Example manual for University of Toronto Simulation (UT-SIM) Framework. (Second edition). *Technical Report, International Workshop on Hybrid Simulation*, Department of Civil Engineering, University of Toronto, Canada.

[25] Mortazavi, P., Huang, X., Kwon, O., Christopoulos, C. (2017): An overview of the University of Toronto Simulation (UT-SIM) Framework and its application to the performance assessment of structures, *Proceedings of the 7th International Conference on Advances in Experimental Structural Engineering*, Pavia, Italy.

[26] Mojiri, S., Kwon, O., Christopoulos, C. (2019): Development of a ten-element hybrid simulation platform and an adjustable yielding brace for performance evaluation of multi-story braced frames subjected to earthquakes, *Journal of Earthquake Engineering and Structural Dynamics*, **48**(7), 749-771, https://doi.org/10.1002/eqe.3155

[27] Mojiri, S., Mortazavi, P., Kwon, O., Christopoulos, C. (2017): Multi-element pseudo-dynamic hybrid simulation of concentric braced frames, *Proceedings of the 7th International Conference on Advances in Experimental Structural Engineering*, Pavia, Italy.

[28] Mojiri, S., Mortazavi, P., Kwon, O., Christopoulos, C: Multi-element pseudo-dynamic testing of concentrically braced frames under earthquake loads, *ASCE Journal of Structural Engineering.* (Under Review).

